

Self-Assembly and Conformational Changes of Hydrophobin Classes at the Air-Water Interface

Konrad Meister^{†}, Alexander Bäumer[‡], Geza R. Szilvay[§], Arja Paananen[§] & Huib J. Bakker[†]*

[†]FOM-Institute for Atomic and Molecular Physics AMOLF, Science Park 104, 1098 XG
Amsterdam, The Netherlands

[‡]Physical Chemistry II, Ruhr University Bochum, Universitätsstr. 150, 44801 Bochum, Germany

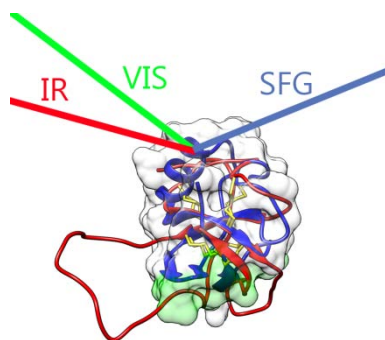
[§]VTT Technical Research Centre of Finland Ltd, Tietotie 2, FI-02150 Espoo, Finland

AUTHOR INFORMATION

Corresponding Author

*K.Meister@amolf.nl

Abstract: We use surface-specific vibrational sum-frequency generation spectroscopy (VSFG) to study the structure and self-assembling mechanism of the class I hydrophobin SC3 from *Schizophyllum commune* and the class II hydrophobin HFBI from *Trichoderma reesei*. We find that both hydrophobins readily accumulate at the water-air interface and form rigid, highly-ordered protein films that give rise to prominent VSFG signals. We identify several resonances that are associated with β -sheet structures and assign them to the central β -barrel core present in both proteins. Differences between the hydrophobin classes are observed in their interfacial self-assembly. For HFBI we observe no changes in conformation upon adsorption to the water surface. For SC3 we observe an increase in β -sheet specific signals that supports a surface-driven self-assembly mechanism in which the central β -barrel remains intact and stacks into a larger-scale architecture, amyloid-like rodlets.



KEYWORDS Hydrophobins, Chiral Sum-Frequency Generation Spectroscopy, Amyloid Formation, Air-Water Interface

Hydrophobins are a group of surface active proteins that are mostly produced by filamentous fungi and that are known for their extraordinary interfacial functions¹. Hydrophobins reduce the surface tension of water, adhere to surfaces, and form protective surface coatings, all functions that play an important role in fungal physiology^{2,3}. The remarkable interfacial properties of hydrophobin films have led to several industrial applications including foams and functional coatings⁴. All these applications rely on the unique surface properties of hydrophobins and a more detailed knowledge of the structure of hydrophobins at the surface could allow for an augmentation of their function and accelerate the development of novel materials and technologies¹. Hydrophobins are generally divided into class I and class II proteins based on their solubility and hydrophathy patterns⁵. The structure of the class II hydrophobins HFBI, HFBI and NC2 has been successfully resolved using X-ray crystallography, and the conformation of some class I hydrophobins have been resolved with NMR⁶⁻⁸. Both hydrophobin classes share a similar fold that consists of a four-stranded β -barrel which is stabilized by intramolecular disulfide bonds as shown in figure 1. In addition, the proteins have a large solvent-exposed hydrophobic patch that renders them amphiphilic. Structural differences between the classes primarily occur in the loop regions of the β -barrel where class I hydrophobins show more variation in length and structure.

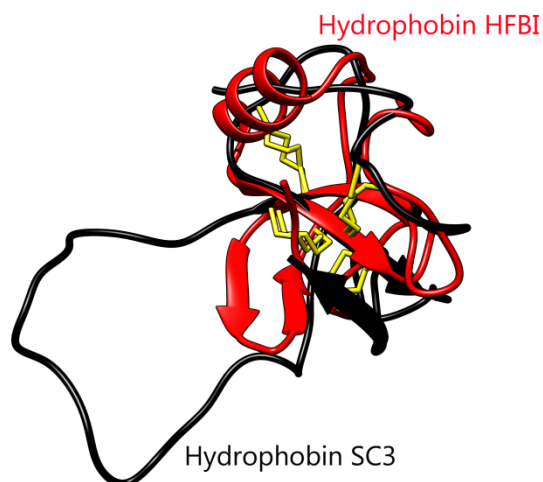


Figure 1. Structural superimposition of the predicted structure of class I hydrophobin SC3 (red) and the crystal structure of the class II hydrophobin HFBI (black). Both proteins share a central β -barrel core that is stabilized by intramolecular disulfide bonds (yellow). Structural differences occur in the loop regions where HFBI does not possess disordered loop regions that are present in SC3.

At the air-water interface both classes self-assemble into stable films with exceptional properties⁹⁻¹⁴. Interestingly, the surface film structure of the similarly folded proteins varies considerably¹⁵. Class I hydrophobins self-assemble into functional amyloid-like structures known as rodlets which associate laterally to form amphipathic, fibrillar layers. Class II hydrophobins form films with a hexagonal structure and distinct repeating units that lack fibrillar structure^{9,10,16}. For class I hydrophobins the conversion into rodlet structures was reported to involve conformational changes and structural intermediates while no such changes were reported for class II hydrophobins¹⁵.

However, the reported experimental data stems from bulk solution studies or were derived from films that were transferred to solid support substrates^{12,13,15}. Due to a lack of surface-

specific molecular probing techniques in solution, only limited information is available on the interfacial self-assembly mechanism. As a result, it is not clear if and where secondary structure changes are taking place in the self-assembly of hydrophobin films.

Here we investigate the film formation of class I hydrophobin SC3 secreted from *S. commune* and the class II hydrophobins HFBI from *T. reesei* using vibrational sum-frequency generation spectroscopy (VSFG). VSFG is a highly surface specific technique that is ideally suited for investigating molecules adsorbed at interfaces¹⁷. In VSFG an infrared light pulse and a visible pulse are combined to generate light at their sum-frequency. The generation is enhanced in case the infrared light is resonant with a molecular vibration. For the bulk the generation of sum-frequency is symmetry forbidden. VSFG has been successfully used to investigate proteins at various interfaces and can provide information on the molecular orientation, conformation and hydration shell of the molecule of interest¹⁸⁻²³.

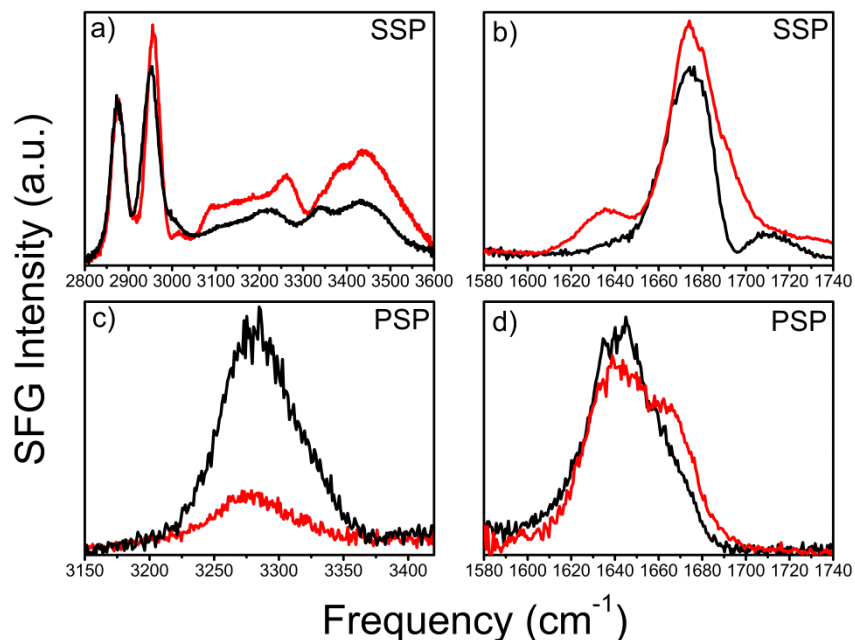


Figure 2. VSFG spectra of aged 15 μM solutions of the class I hydrophobin SC3 (pH 7, 20 $^{\circ}\text{C}$) (red) and the class II hydrophobin HFBI (pH 7, 20 $^{\circ}\text{C}$) (black) at the water-air surface measured in the SSP and the PSP polarization configuration. (a) VSFG spectra of SC3 (red) and HFBI (blue) contain contributions from C-H, N-H and O-H stretching vibrations. (b) VSFG spectra in the amide I region contain a dominant peak centered at $\sim 1675\text{ cm}^{-1}$ (c-d) In the PSP spectra both hydrophobins show signals centered at $\sim 3270\text{ cm}^{-1}$ and $\sim 1640\text{ cm}^{-1}$ that originate from β -structures.

Figure 2a-d shows VSFG spectra of aged solutions of HFBI and SC3 in water (pH 7, 20 $^{\circ}\text{C}$) at the air/water interface, measured in the SSP (s-SFG, s-VIS, p-IR) and PSP (p-SFG, s-VIS, p-IR) polarization configuration. In the C-H stretch region several signals are identified that are associated with the hydrophobin films. We assign these bands to the methyl symmetric stretch ($\sim 2870\text{ cm}^{-1}$), a Fermi resonance ($\sim 2940\text{ cm}^{-1}$) and aromatic C-H stretch ($\sim 3060\text{ cm}^{-1}$) vibrations²⁴. In the broad O-H stretch region we attribute resonances at $\sim 3250\text{ cm}^{-1}$ and ~ 3400 -

3450 cm^{-1} to interfacial water. The SSP spectra of class I and class II hydrophobins, shown in Figure 2a, show additional features (dips) near 3300 cm^{-1} and 3370 cm^{-1} . These signals have a negative sign and are asymmetric due to the interference with the strong signal of the O-H stretching modes. We performed additional pH-dependent VSFG measurements (Supporting Figure 1) to clarify the frequency position and spectra shape of these signals. At low pH, the dips turn into clear positive signals at 3310 and 3370 cm^{-1} , reflecting a change in phase between these signals and the strong signal of the O-H stretch vibrations. We assign the signals observed at 3310 cm^{-1} and 3370 cm^{-1} to N-H bands originating from the protein backbone and amide containing side chains.²⁵

In figure 2b we show VSFG spectra of the two hydrophobins in the amide I region. For both proteins we observe a strong signal centered at $\sim 1675 \text{ cm}^{-1}$. We assign this band to a combination of a β -turn band (typically centered at $\sim 1665 \text{ cm}^{-1}$) and an antiparallel β -sheet mode (B_1 -mode, typically centered at $\sim 1685 \text{ cm}^{-1}$) that originate from the central β -barrel structure, present in both hydrophobins^{18,26,27}. We observe a weaker band at $\sim 1635 \text{ cm}^{-1}$ that we assign to the B_2 -mode of the antiparallel β -sheets²⁶. By measuring VSFG spectra with PSP polarization configuration, we can specifically probe the chiral vibrations of hydrophobin. Thereby VSFG spectra in PSP provide valuable information on the chirality of the molecules, and can be used to identify specific secondary structure elements of proteins at interfaces^{28, 29}.

The chiral VSFG spectra of both hydrophobins are shown in figure 2c-d. In the amide I region, strong chiral VSFG signals result from β -sheet secondary structures^{28, 30}. We assign the signal at $\sim 1640 \text{ cm}^{-1}$ to the antiparallel β -sheet B_2 mode and the shoulder at $\sim 1666 \text{ cm}^{-1}$ to β -turn elements present in the central β -barrel of hydrophobins^{27,30}. This peak assignment agrees well with recent findings of a bacterial biofilm protein with a similar tertiary structure²⁷. We thus find that the

achiral and chiral VSFG spectra show similar bands in the amide region, but with different intensities due the different selection rules associated with SSP and PSP polarization configurations. Both chiral and achiral VSFG spectra contain a clear contribution of the 1665 cm^{-1} band of the β -turn elements. According to the orientation analysis of interfacial antiparallel β -sheet structures reported by Nguyen *et al.*, the B_2 -mode (the $\sim 1640 \text{ cm}^{-1}$ peak) should be stronger than the B_1 -mode, both in SSP and PSP¹⁸. This agrees with the observations for the PSP (chiral) VSFG spectrum. For the SSP (achiral) VSFG spectrum the situation is more complex, because the 1675 cm^{-1} band contains contributions from both the B_1 -mode and the β -turn modes. The observed higher intensity of the $\sim 1675 \text{ cm}^{-1}$ band (B_1 -mode + β -turn modes) compared to the $\sim 1675 \text{ cm}^{-1}$ band (the B_2 -mode) in the achiral VSFG spectrum, suggests that the B_1 -mode forms only a minor contribution to the 1675 cm^{-1} band, and that this band is dominated by the response of the β -turn modes of the hydrophobin.

Chiral signals in the region from 3270-3300 cm^{-1} have previously been assigned to the N-H vibrations of both helical and β -sheet secondary structures²¹. In the crystal structure of HFBI a helical segment is present while for SC3 no helical structures are present. We thus assign the signal at $\sim 3270 \text{ cm}^{-1}$ to N-H vibrations found in antiparallel β -sheet structures²⁵. The frequency of 3270 cm^{-1} differs from the frequencies of the N-H vibrations that are observed in the VSFG spectra measured in SSP polarization configuration (Figure 2a). This difference can be explained from the fact that only the chiral N-H vibrations (arranged via secondary structural elements) will be observed in VSFG spectra measured in PSP. If these latter N-H vibrations are engaged in relatively strong hydrogen-bonded structures, the resulting frequency of these N-H modes will be lower than the frequencies of the average N-H vibrations that are probed in SSP. We also notice that the N-H band at 3270 cm^{-1} is slightly asymmetric. Due to the absence of a strong non-

resonant background in the PSP configuration, this suggests that a second, higher-frequency band could be present which may correspond to the chiral β -turn structure that is also observed in the chiral amide I spectra.

The observation of chiral VSG signals proves that the SFG active elements of the secondary structure of both hydrophobins remain in a folded state at the interface, as unfolding of these SFG active elements would inevitably lead to a loss of the chiral VSG response.

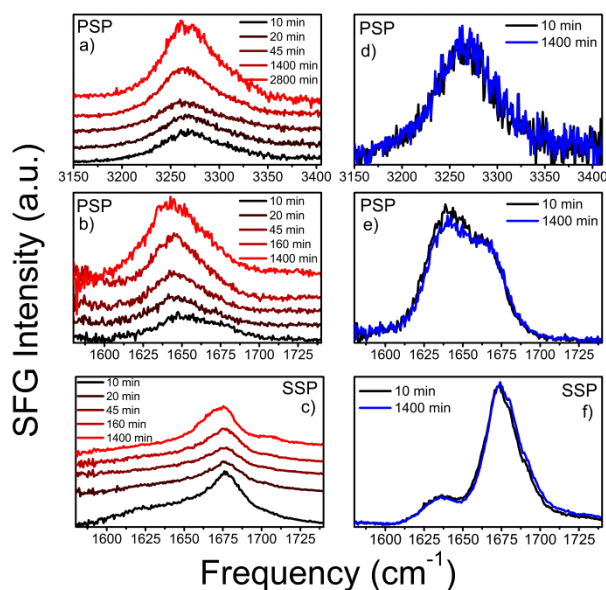


Figure 3. Time-dependence of the VSG spectra of the class I hydrophobin SC3 (red) and class II hydrophobin HFBI (blue) at the air-water interface measured in SSP and PSP polarization configuration. (a-b) In the cVSG spectra of SC3 (measured with PSP) the main signals at $\sim 3270\text{ cm}^{-1}$ and $\sim 1640\text{ cm}^{-1}$ significantly gain intensity over time. (c) The main VSG signal of SC3 centered at $\sim 1675\text{ cm}^{-1}$ (measured with SSP) first decreases in intensity and then increases again after several hours. (d-f) For the class II HFBI we observe no spectral changes over time.

Figure 3 presents the time-dependence of VSG spectra of freshly prepared 25 μM SC3 and HFBI solutions (50 mM phosphate buffer, pH 7) in the amide I and N-H stretch region using the SSP and PSP polarization configuration. These time-dependent spectra provide information on the kinetics and spectral changes of the hydrophobin assembly at the interface between $t=0$ and 1400 min. We used a Rochon-Polarizer to simultaneously measure spectra in the SSP and PSP polarization configuration to ensure that identical self-assembly processes are monitored in both polarization configurations³¹.

For the class I hydrophobin SC3 we observe that in the SSP spectra (Figure 3c) the pronounced shoulder that is present at the beginning of the time series at $\sim 1635\text{-}1655\text{ cm}^{-1}$ loses intensity over time and completely disappears at the end of the time series. The PSP spectra of SC3 in Figure 3b-c show a gradual increase in intensity for both the amide I band at $\sim 1640\text{ cm}^{-1}$ and the N-H band at $\sim 3270\text{ cm}^{-1}$. Both peaks are characteristic of β -sheet structures and indicate a gradual built-up of chiral β -sheet structures at the air-water interface. It is also worth mentioning that after several hours some scattering from the SC3 samples was observed, suggesting the presence of large-scale particles such as rodlets. The time-dependent measurements of the class II hydrophobin HFBI showed negligible spectral changes and the SSP and PSP VSG spectra taken after 10 minutes and 1400 min are almost indistinguishable as shown in figure 3d-f.

Hydrophobins readily self-assemble and form stable, highly-ordered protein monolayers at the air-water interface¹. We find that the class I hydrophobin SC3 and class II hydrophobin HFBI show similar SSP and PSP VSG spectra, which proves that on the molecular level both proteins share comparable β -sheet rich structures at the air-water interface. We assign the observed amide and N-H bands predominantly to the central β -barrel core found in their solution structures, and

conclude that the central β -barrel remains intact upon adsorption to the interface. We used VSFG spectra to monitor the time-dependence of the self-assembly of both hydrophobin classes at the water surface. We observed no spectral changes during the adsorption and self-assembly of HFBI and conclude that neither is accompanied by a change in secondary structure. This finding agrees with previous studies that e.g. showed that the lowering of the water surface tension through HFBI occurred almost instantly¹⁵.

In contrast to HFBI we observed spectral changes during the self-assembly of SC3 that provide evidence for conformational alterations at the interface. At the early stages of the SC3 adsorption and self-assembly we observed a decrease in the SSP amide I signals around ~ 1630 - 1650 cm^{-1} . We assign these spectral changes to conformational changes that can involve α -helical or random coil intermediates, but which cannot be distinguished due to the spectral overlap of their amide I signatures³². We did not find such changes during HFBI adsorption and conclude that the conformational changes observed for SC3 likely occur in the extended loop regions as these are absent in class II hydrophobins like HFBI. This finding agrees very well with the results of a molecular dynamics simulation study of SC3 that proposed conformational changes in the loop region between the third and fourth cysteine residue, while the percentage of the β -sheets within a monomer remains effectively constant³³.

We further observed a significant increase in β -sheet specific signals during the SC3 self-assembly, as shown in figure 4. Circular dichroism (CD), thioflavin T fluorescence, attenuated-total reflectance-Fourier transform infrared (ATR-FTIR), and fiber diffraction data all point towards an increase of the amount of β -structures upon film formation at hydrophobic-hydrophilic interfaces^{8,13,34}. These results were explained either by ordering of the existing β -structures upon assembly or by the adoption of a new β -sheet rich conformation by the

disordered loops. We explain the observed signal amplification from the stacking of SC3 monomers to characteristic amyloid-like rodlet structures, as shown in figure 4. The stacking increases the order of the hydrophobin films at the interface and gives rise to amplified VSG signals as these signals increase with increasing molecular order. The absence of an increase of the VSG signal for HFBI can be well explained from the fact that class II hydrophobins do not form amyloid like rods, but instead form films with a hexagonal structure and distinct repeating units that lack fibrillar structure^{13,35}.

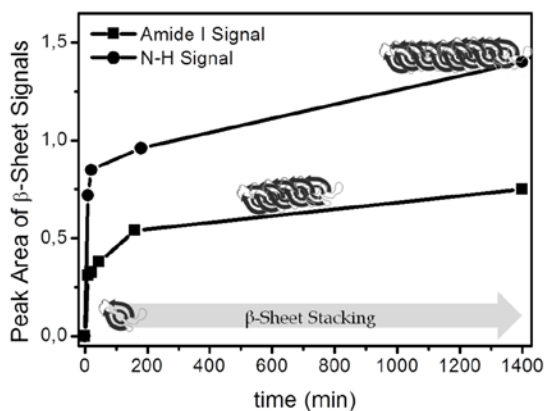


Figure 4. Schematic representation of SC3 monomer stacking at the air-water interface. The amplitudes of $v_{N-H, PSP}$ and $v_{PSP, Amide I}$ as a function of time during SC3 assembly at the air-water interface. The solid lines represent a guide to the eye.

In summary, we used VSFG to probe the self-assembly mechanism of different hydrophobin classes. In the top molecular layers, as probed by VSFG, the spectral signature of both proteins is similar and rich in β -sheet structures. Our findings reveal that the class I hydrophobin SC3 and the class II hydrophobin HFBI have different self-assembling mechanism in agreement with earlier studies in which the surface region was probed over a much larger depth. We propose a self-assembly mechanism for class I hydrophobins in which the defined β -sheet core remains

intact within a larger-scale architecture, amyloid rodlets³⁵. The ordering of the β -sheet cores resulting from the rodlet formation leads to a strong enhancement of the chiral VSFG signals of the amide and N-H stretch vibrations.

ASSOCIATED CONTENT

SUPPORTING INFORMATION (SI)

Supporting Information Available:

Experimental details of the VSFG setup and the measurement procedure, text and figure explaining the interferences and assignment of the achiral N-H signals, This material is available free of charge via the internet <http://pubs.acs.org>.

AUTHOR INFORMATION

Corresponding Author

*Email: K.Meister@amolf.nl

Notes

The authors declare no competing financial interests.

ACKNOWLEDGMENT

This work is part of the research program of the Foundation for Fundamental Research on Matter (FOM), which is part of the Netherlands Organisation for Scientific Research (NWO). K. M. gratefully acknowledges the European Commission for funding through the award of a Marie Curie fellowship. A. B. acknowledges support by the Cluster of Excellence RESOLV (EXC

1069) funded by the Deutsche Forschungsgemeinschaft. A.P. and G.R.S. acknowledges support by the Academy of Finland through its Centres of Excellence Programme (2014-2019). Riitta Suihkonen is thanked for technical assistance with hydrophobins.

REFERENCES

- (1) Linder, M. B., Hydrophobins: Proteins that Self-Assemble at Interfaces. *Curr. Opin. Colloid Interface Sci.* **2009**, *14*, 356-363.
- (2) Wösten, H. A. B.; de Vocht, M. L., Hydrophobins, the Fungal Coat Unravelled. *Biochim. Biophys. Acta, Biomembr.* **2000**, *1469*, 79-86
- (3) Wösten, H. A. B.; van Wetter, M.-A.; Lugones, L. G.; van der Mei, H. C.; Busscher, H. J.; Wessels, J. G. H., How a Fungus Escapes the Water to Grow into the Air. *Curr. Biol.* **1999**, *9*, 85-88.
- (4) Wösten, H. B.; Scholtmeijer, K., Applications of Hydrophobins: Current State and Perspectives. *Appl. Microbiol. Biotechnol.* **2015**, *99*, 1587-1597.
- (5) Wessels, J. G. H., Developmental Regulation of Fungal Cell Wall Formation. *Annu. Rev. Phytopathol.* **1994**, *32*, 413-437.
- (6) Hakanpää, J.; Paananen, A.; Askolin, S.; Nakari-Setälä, T.; Parkkinen, T.; Penttilä, M.; Linder, M. B.; Rouvinen, J., Atomic Resolution Structure of the HFBII Hydrophobin, a Self-assembling Amphiphile. *J. Biol. Chem.* **2004**, *279*, 534-539

- (7) Hakanpää, J.; Szilvay, G. R.; Kaljunen, H.; Maksimainen, M.; Linder, M.; Rouvinen, J., Two Crystal Structures of *Trichoderma reesei* Hydrophobin HFBI--the Structure of a Protein Amphiphile with and without Detergent Interaction. *Protein Sci.* **2006**, *15*, 2129-40
- (8) Kwan, A. H.; Winefield, R. D.; Sunde, M.; Matthews, J. M.; Haverkamp, R. G.; Templeton, M. D.; Mackay, J. P., Structural Basis for Rodlet Assembly in Fungal Hydrophobins. *Proc. Natl. Acad. Sci. U.S.A.*, **2006**, *103*, 3621-3626.
- (9) Paananen, A.; Vuorimaa, E.; Torkkeli, M.; Penttilä, M.; Kauranen, M.; Ikkala, O.; Lemmetyinen, H.; Serimaa, R.; Linder, M. B., Structural Hierarchy in Molecular Films of Two Class II Hydrophobins. *Biochemistry* **2003**, *42*, 5253-5258
- (10) Szilvay, G. R.; Paananen, A.; Laurikainen, K.; Vuorimaa, E.; Lemmetyinen, H.; Peltonen, J.; Linder, M. B., Self-Assembled Hydrophobin Protein Films at the ~~A~~Water Interface: Structural Analysis and Molecular Engineering. *Biochemistry* **2007**, *46*, 2345-2354
- (11) Lienemann, M.; Grunér, M. S.; Paananen, A.; Siika-aho, M.; Linder, M. B., Charge-Based Engineering of Hydrophobin HFBI: Effect on Interfacial Assembly and Interactions. *Biomacromolecules*, **2015**, *16*, 1283-1292
- (12) Macindoe, I.; Kwan, A. H.; Ren, Q.; Morris, V. K.; Yang, W.; Mackay, J. P.; Sunde, M., Self-Assembly of Functional, Amphipathic Amyloid Monolayers by the Fungal Hydrophobin EAS. *Proc. Natl. Acad. Sci. U.S.A.*, **2012**, *109*, 804-811
- (13) De Vocht, M. L.; Reviakine, I.; Ulrich, W.-P.; Bergsma-Schutter, W.; Wösten, H. A. B.; Vogel, H.; Brisson, A.; Wessels, J. G. H.; Robillard, G. T., Self-Assembly of the Hydrophobin SC3 Proceeds via Two Structural Intermediates. *Protein Sci.* **2002**, *11*, 1199-1205

- (14) Magarkar, A.; Mele, N.; Abdel-Rahman, N.; Butcher, S.; Torkkeli, M.; Serimaa, R.; Paananen, A.; Linder, M.; Bunker, A., Hydrophobin Film Structure for HFBI and HFBII and Mechanism for Accelerated Film Formation. *PLoS Comput. Biol.* **2014**, *10*, e1003745
- (15) Askolin, S.; Linder, M.; Scholtmeijer, K.; Tenkanen, M.; Penttilä, M.; de Vocht, M. L.; Wösten, H. A. B., Interaction and Comparison of a Class I Hydrophobin from *Schizophyllum commune* and Class II Hydrophobins from *Trichoderma reesei*. *Biomacromolecules* **2006**, *7*, 1295-1301
- (16) Ren, Q.; Kwan, A. H.; Sunde, M., Solution Structure and Interface-Driven Self-Assembly of NC2, a New Member of the Class II Hydrophobin Proteins. *Proteins* **2014**, *82*, 990-1003
- (17) Shen, Y. R., Surface Properties probed by Second-Harmonic and Sum-Frequency Generation. *Nature* **1989**, *337*, 519-525
- (18) Nguyen, K. T.; King, J. T.; Chen, Z., Orientation Determination of Interfacial β -Sheet Structures in Situ. *J. Phys. Chem. B*, **2010**, *114*, 8291-8300
- (19) Meister, K.; Strazdaite, S.; DeVries, A. L.; Lotze, S.; Olijve, L. L.C.; Voets, I. K.; Bakker, H. J. Observation of Ice-Like Water Layers at an Aqueous Protein Surface *Proc. Natl. Acad. Sci. U.S.A.* **2014**, *111*, 11372–11376
- (20) Meister, K.; Lotze, S.; Olijve, L. L. C.; DeVries, A. L.; Duman, J. G.; Voets, I. K.; Bakker, H. J., Investigation of the Ice-Binding Site of an Insect Antifreeze Protein Using Sum-Frequency Generation Spectroscopy. *J. Phys. Chem. Lett.* **2015**, *6*, 1162-1167
- (21) Yan, E. C. Y.; Fu, L.; Wang, Z.; Liu, W. Biological Macromolecules at Interfaces Probed by Chiral Vibrational Sum Frequency Generation Spectroscopy. *Chem. Rev.* **2014**, *114*, 8471-8498

- (22) Chen, X.; Wang, J.; Sniadecki, J. J.; Even, M. A.; Chen, Z., Probing α -Helical and β -Sheet Structures of Peptides at Solid/Liquid Interfaces with SFG. *Langmuir* **2005**, *21*, 2662-2664
- (23) Engelhardt, K.; Peukert, W.; Braunschweig, B., Vibrational Sum-Frequency Generation at Protein Modified Air–Water Interfaces: Effects of Molecular Structure and Surface Charging. *Curr. Opin. Colloid Interface Sci.* **2014**, *19*, 207-215
- (24) Conboy, J. C.; Messmer, M. C.; Richmond, G. L., Dependence of Alkyl Chain Conformation of Simple Ionic Surfactants on Head Group Functionality As Studied by Vibrational Sum-Frequency Spectroscopy. *J. Phys. Chem. B.* **1997**, *101*, 6724-6733
- (25) Fu, L.; Wang, Z.; Yan, E. C., N-H Stretching Modes around 3300 Wavenumber from Peptide Backbones observed by Chiral Sum Frequency Generation Vibrational Spectroscopy. *Chirality* **2014**, *26*, 521-524
- (26) Ye, L.; Liu, J.; Yan, E. C. Y., Structure and Orientation of Interfacial Proteins Determined by Sum Frequency Generation Vibrational Spectroscopy: Method and Application. *Adv. Protein Chem. Struct. Biol.* **2013**, *93*, 213-255
- (27) Wang, Z et al. A Narrow Amide I Vibrational Band Observed by Sum Frequency Generation Spectroscopy Reveals Highly Ordered Structures of a Biofilm Protein at the Air/Water Interface. *Chem. Comm.* **2016**, *52*, 2956
- (28) Fu, L.; Liu, J.; Yan, E. C. Y., Chiral Sum Frequency Generation Spectroscopy for Characterizing Protein Secondary Structures at Interfaces. *J. Am. Chem. Soc.* **2011**, *133*, 8094-8097

- (29) Yan, E. C. Y.; Wang, Z.; Fu, L., Proteins at Interfaces Probed by Chiral Vibrational Sum Frequency Generation Spectroscopy. *J. Phys. Chem. B.* **2015**, *119*, 2769-2785
- (30) Fu, L.; Xiao, D.; Wang, Z.; Batista, V. S.; Yan, E. C. Y., Chiral Sum Frequency Generation for In Situ Probing Proton Exchange in Antiparallel β -Sheets at Interfaces. *J. Am. Chem. Soc.* **2013**, *135*, 3592-3598
- (31) McDermott, M. L.; Petersen, P. B., Robust Self-Referencing Method for Chiral Sum Frequency Generation Spectroscopy. *J. Phys. Chem. B.* **2015**, *119*, 12417-12423
- (32) Barth, A.; Zscherp, C., What Vibrations Tell us about Proteins. *Q. Rev. Biophys.* **2002**, *35*, 369-430
- (33) Fan, H.; Wang, X.; Zhu, J.; Robillard, G. T.; Mark, A. E., Molecular Dynamics Simulations of the Hydrophobin SC3 at a Hydrophobic/Hydrophilic Interface. *Proteins* **2006**, *64*, 863-73
- (34) Butko, P.; Buford, J. P.; Goodwin, J. S.; Stroud, P. A.; McCormick, C. L.; Cannon, G. C., Spectroscopic Evidence for Amyloid-Like Interfacial Self-Assembly of Hydrophobin SC3. *Biochem. Biophys. Res. Commun.* **2001**, *280*, 212-215
- (35) Morris, V. K.; Linser, R.; Wilde, K. L.; Duff, A. P.; Sunde, M.; Kwan, A. H., Solid-State NMR Spectroscopy of Functional Amyloid from a Fungal Hydrophobin: A Well-Ordered β -Sheet Core Amidst Structural Heterogeneity. *Angew. Chem.* **2012**, *51*, 12621-12625

Supporting Information

Self-Assembly and Conformational Changes of Hydrophobin Classes at the Air-Water Interface

Konrad Meister^{†}, Alexander Bäumer[‡], Geza R. Szilvay[§], Arja Paananen[§] & Huib J. Bakker[†]*

[†]FOM-Institute for Atomic and Molecular Physics AMOLF, Science Park 104, 1098 XG
Amsterdam, The Netherlands

[‡]Physical Chemistry II, Ruhr University Bochum, Universitätsstr. 150, 44801 Bochum,
Germany

[§]VTT Technical Research Centre of Finland Ltd, Tietotie 2, FI-02150 Espoo, Finland

Material and Methods:

The laser source for the VSFG setup is a regenerative Ti:Sapphire amplifier (Coherent) producing 800 nm pulses at a 1 kHz repetition rate with a pulse duration of 35 fs and a pulse energy of 3.5 mJ. Approximately one third of the laser output is used to pump a home-built optical parametric amplifier and a difference-frequency mixing stage. This nonlinear optical device produces tuneable broadband mid-IR pulses (ranging from 2-10 μm , 600 cm^{-1} bandwidth at FWHM, 10-20 μJ). The IR pulses have a sufficiently large bandwidth to measure the complete VSFG spectrum of the OH (OD) stretch vibrations of H_2O (D_2O). Another part of the 800 nm pulse is sent through an etalon to narrow down its bandwidth to $\sim 15 \text{ cm}^{-1}$. The resulting narrow-band 800 nm pulse (VIS) and the broadband IR pulse are directed to the sample surface at angles of $\sim 50^\circ$ and $\sim 55^\circ$, respectively, to generate light at the sum frequency. The VIS and IR beams are focused in spatial and temporal overlap on the sample surface with 200 mm and 100 mm focal length lenses, respectively. The VSFG light generated at the surface is sent to a monochromator and detected with an Electron-Multiplied Charge Coupled Device (EMCCD, Andor Technologies).

Chiral VSFG measurements were performed with p-polarised IR or p-polarised SFG, s-polarised VIS, and p-polarised IR (with respect to the plane of incidence). We used a Rochon-Polarizer that enables the simultaneous detection of both chiral and achiral VSFG signals¹. The typical acquisition time of the VSFG spectra in the SSP and PSP polarization configuration is 600 seconds. Spectra are first background subtracted (blocked IR) and normalized to a reference SFG spectrum measured from z-cut quartz. All experimental data shown are raw data.

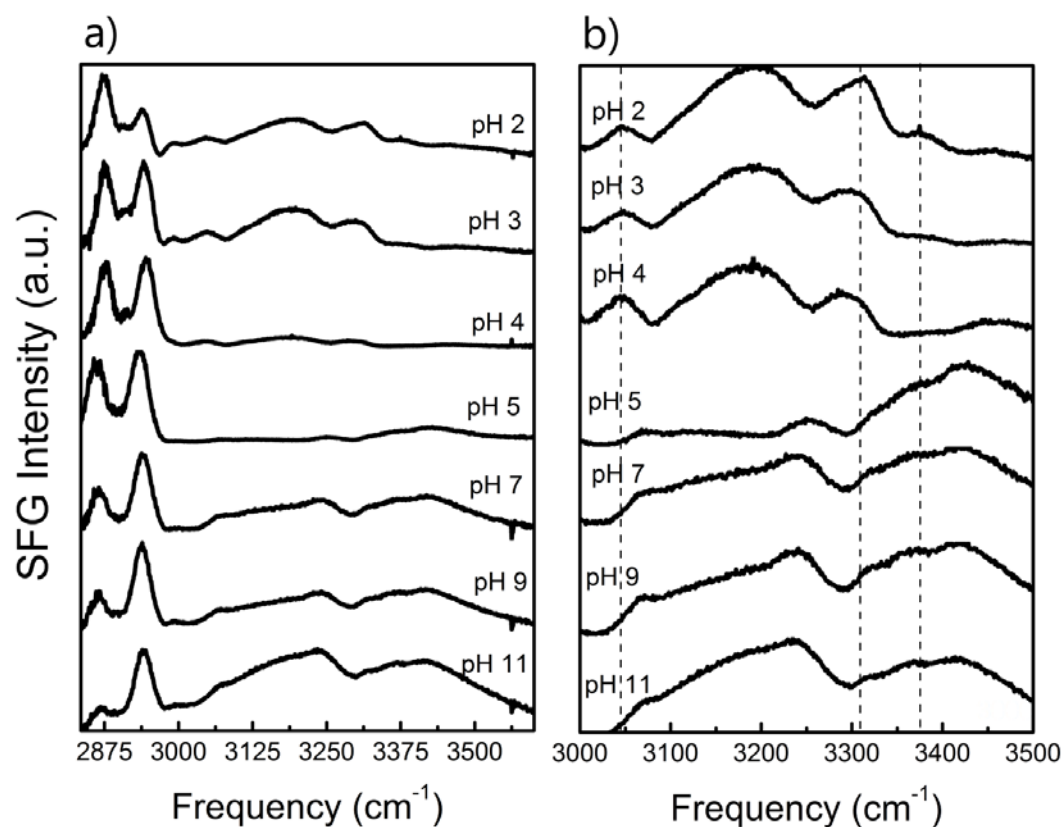
The measurements were performed using H₂O (Millipore), D₂O or phosphate buffer solutions (50 mM phosphate, pH 7). The pH (Mettler Toledo FE20) of the samples was routinely checked before and after each measurement.

Class II hydrophobins HFBI were provided by VTT research and purified as described in detail elsewhere^{2,3}. HFBI was purified by aqueous two-phase separation (ATPS) and purified further by preparative reversed-phase chromatography using a Vydac C4 column and a gradient elution from 0.1% trifluoroacetic acid (TFA) to 100% acetonitrile (ACN) containing 0.1% trifluoroacetic acid. The protein sample was eluted as a single peak, and after evaporation of ACN and TFA, the peak fractions were pooled and lyophilized. The purity level is $\geq 98\%$. Class I hydrophobin SC3 (purity $\geq 98\%$) was purchased from Sigma Aldrich and used without further purification. For the results shown in figure 2 the hydrophobin samples were prepared several hours before the measurements to account for the effect that hydrophobin HFBI and SC3 need different times to reach equilibrium at the air-water interface. For the time-lapse VSFG experiments we used freshly prepared samples and experimental conditions that were identical to those used in the study from De Vocht *et al*⁴. 5 ml of a freshly prepared 0.2 mg/ml ($\sim 27\mu\text{M}$) hydrophobin solution (50 mM phosphate, pH 7) in H₂O or D₂O was added in a Teflon trough and spectra recording was started immediately.

Interference and assignment of the N-H signals:

It is well-established that pH-induced changes in the C-H signals of proteins in conventional VSFG spectra are largely due to a change of the phase difference between the C-H and O-H signals rather than a change of the character of the C-H stretch vibrations⁵. In several VSFG studies of proteins the aromatic C-H stretching band at $\sim 3050\text{ cm}^{-1}$ was used to deduce the absolute water orientation at the protein/water interface by considering its interference with the broad hydrogen-bonded water band⁶. While the influence on the C-H vibration is well

known, little information currently exist on the interference with the N-H vibrational bands which are typically covered by the broad O-H region. We find that the modes of the N-H stretching vibrations at $\sim 3310\text{ cm}^{-1}$ and $\sim 3370\text{ cm}^{-1}$ change in a similar way as the aromatic C-H vibration at $\sim 3050\text{ cm}^{-1}$. As illustrated in Figures S1, at pH values below the IEP the bands appear as positive peaks while for pH values above the IEP negative features are observed.



Supporting Figure 1. (a) Vibrational SFG spectra of the class II hydrophobin HFBI adsorbed at the air-water interface, measured in SSP polarization configuration. Spectra were taken at different pH values as indicated. (b) Magnification of the changes in the signals at $\sim 3050\text{ cm}^{-1}$ and 3310 cm^{-1} and 3370 cm^{-1} .

References

- (1) McDermott, M. L.; Petersen, P. B., Robust Self-Referencing Method for Chiral Sum Frequency Generation Spectroscopy. *J. Phys. Chem. B.* **2015**, *119*, 12417-12423
- (2) Paananen, A.; Vuorimaa, E.; Torkkeli, M.; Penttilä, M.; Kauranen, M.; Ikkala, O.; Lemmetyinen, H.; Serimaa, R.; Linder, M. B., Structural Hierarchy in Molecular Films of Two Class II Hydrophobins. *Biochemistry* **2003**, *42*, 5253-5258
- (3) Hakanpää, J.; Szilvay, G. R.; Kaljunen, H.; Maksimainen, M.; Linder, M.; Rouvinen, J., Two Crystal Structures of Trichoderma Reesei Hydrophobin HFBI--the Structure of a Protein Amphiphile with and without Detergent Interaction. *Protein. Sci.* **2006**, *15*, 2129-2140
- (4) De Vocht, M. L.; Reviakine, I.; Ulrich, W.-P.; Bergsma-Schutter, W.; Wösten, H. A. B.; Vogel, H.; Brisson, A.; Wessels, J. G. H.; Robillard, G. T., Self-Assembly of the Hydrophobin SC3 Proceeds via Two Structural Intermediates. *Protein. Sci.* **2002**, *11*, 1199-1205
- (5) Wang, J.; Buck, S. M., Chen, Z., Sum Frequency Generation Vibrational Spectroscopy Studies on Protein Adsorption, *J. Phys. Chem. B.*, **2002**, *106*, 11666-11672
- (6) Engelhardt, K.; Peukert, W.; Braunschweig, B., Vibrational sum-frequency generation at protein modified air–water interfaces: Effects of molecular structure and surface charging. *Curr. Opin. Colloid Interface Sci.* , **2014**, *19*, 207-215